ACCURACY OF LINEAR DEPOLARISATION RATIOS IN CLEAN AIR RANGES MEASURED WITH POLIS-6 AT 355 AND 532 NM

Volker Freudenthaler[1]*, Meinhard Seefeldner[1], Silke Groß[2], Ulla Wandinger[3]

*[1]Ludwig-Maximilians-Universität, Meteorologisches Institut, Theresienstr. 37, 80333 Munich, Germany, *Email: volker.freudenthaler@lmu.de*

[2]DLR, Insitut für Physik der Atmosphäre, 82234 Oberpaffenhofen, Germany

[3]Leibniz Institute for Tropospheric Research (TROPOS), Permoserstr. 15, 04318 Leipzig, Germany,

ABSTRACT

Linear depolarization ratios in clean air ranges were measured with POLIS-6 at 355 and 532 nm. The mean deviation from the theoretical values, including the rotational Raman lines within the filter bandwidths, amounts to 0.0005 at 355 nm and to 0.0012 at 532 nm. The mean uncertainty of the measured linear depolarization ratio of clean air is about 0.0005 at 355 nm and about 0.0006 at 532 nm.

1. INTRODUCTION

Large errors of the linear depolarization ratio (LDR, δ) result from the use of uncertain atmospheric reference values in the relative calibration of the two polarization channels [1]. Several instrumental calibration techniques have been proposed to overcome that, which still can have large uncertainties due to an unknown state of polarization of the emitted laser beam, polarizing optics, rotational misalignment of the optics and of the calibration device, and cross talk of the polarizing beam splitter [2] . In this work we show how those uncertainties have been minimized in the design of POLIS-6, which is a six-channel upgrade of POLIS [3], developed and manufactured by the Meteorological Institute of the LMU in Munich, Germany, in 2013. Furthermore, we show the validation of the measurement accuracy by means of a comparison with theoretically well known LDRs from air molecules.

2. LIDAR SETUP AND SPECIFICATIONS

POLIS-6 is a truly portable lidar system (see Fig. 1) with specifications shown in Tab. 1. It is operated on a tripod and can be pointed to any direction. The desired low distance of full overlap of 70 m requires a large field of view of ±2.5 mrad (tilted slit [4]) and an optimized optical design to keep the optical paths in the receiving optics short. The laser is directly mounted on the rigid telescope tube (see Fig. 1) without any emitter optics, which avoids possible elliptical polarization of the emitted laser beam. The pointing is achieved with a high precision and very stable two-axis tilt mount and controlled with a camera module in place of one of the detector modules.

Table 1 Specifications of POLIS-6

Laser	Nd:YAG Litron LG-250-10
Emitted wavelengths [nm]	355, pol. vertical / 532, pol. horiz.
SHG/THG	KTP II / BBO
Emitted pulse energy	50 / 27 mJ*
Repetition rate	10 Hz
Puls length	4 - 6 ns
Pointing stability	< 70 µrad fw
Beam divergence	<0.5 mrad**
Telescope	Dall-Kirkham
Effective diameter	175 mm
Focal length	1200 mm
Field of view [mrad]	variable, typ. ±2.5
Detection channels	355s, 355p, 387, 532s, 532p, 607
Filter bandwidths: CWL, BW fwhm [nm]	354.6 s&p, 1.1 386.7, 0.52 532.04 s&p, 0.97 607.54, 1.38
Additional polarization-filters: WL (nm), type, extinction ratio	ITOS: 355, XP-38R, 6.4e-4 532, XP-40HT, 2e-4
Data acquisition	6x Licel TR 40-160
Range resolution	3.75 m

* with internal attenuation

** full width (fw) at 90% of output energy

The receiving optics has been selected to yield minimal diattenuation $|D_O|$ with total values (before the polarizing beam splitter cubes (PBC) at 355 and 532 nm, and before the detectors at 387 and 607 nm) smaller than [0.002, 0.032, 0.022, 0.033] at [355, 387, 532, 607] nm, respectively.

Additional polarization filters behind the PBCs eliminate all cross talk. The Δ90°-calibration with mechanical rotation before the receiving optics [2, 3] (see Fig. 1) is used for the relative calibration of the polarization channels. The retardation of the optics can be neglected because the rotational alignment of the receiving optics module can be determined and adjusted with better than 0.5° precision with respect to the laser polarization (see day-to-day variability after 25.06. in Fig. 5).

Figure 1 POLIS-6 with the receiving optics rotated at ±45° (left, right) for the Δ90°-calibration, and at 0° (middle) for atmospheric measurements.

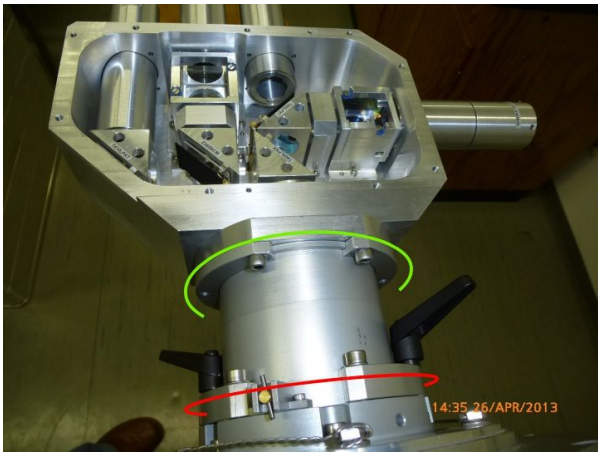

Figure 2 Inside of the receiving optics module of POLIS-6 with the top cover removed. The telescope mount is at the image bottom, indicated by the red circle, which also provides the rotation with the fixed ±45° and 0° positions of the module with respect to the laser/telescope assembly (see Fig.1). The green circle indicates the rotation mount for exact 0° adjustment. At the right and top the detector modules are protruding.

3. THEORY

For the comparison of the measured LDR of clean air ranges with the theoretical values, the rotational Raman lines (RRL) within the bandwidth of the interference filters have to be considered for the calculation of the theoretical molecular (air) LDR. This depends on the bandwidth (BW) and center wavelength (CWL) of the interference filter (IFF) and on the clean air temperature, but also on the exact laser wavelengths. The latter are usually not measured by the laser manufacturers. The fundamental laser wavelength depends, among others, on the temperature of the Nd:YAG rod [5], which we assume for a first estimation to be in the range between 25°C and 85°C. Assuming that the wavelength in air is 1064.15 nm at a rod temperature of 300 K [6] and shifts about +0.005nm/K [5], the second and third harmonics are between 532.07 and 532.22, and 354.71 and 354.81 nm, respectively. While we have measured transmission values for the used 355 nm IFF, we use the specified CWL and BW of the 532 nm IFF (Tab. 1) to calculate the typical two-cavity IFF transmission shape (Fig. 3).

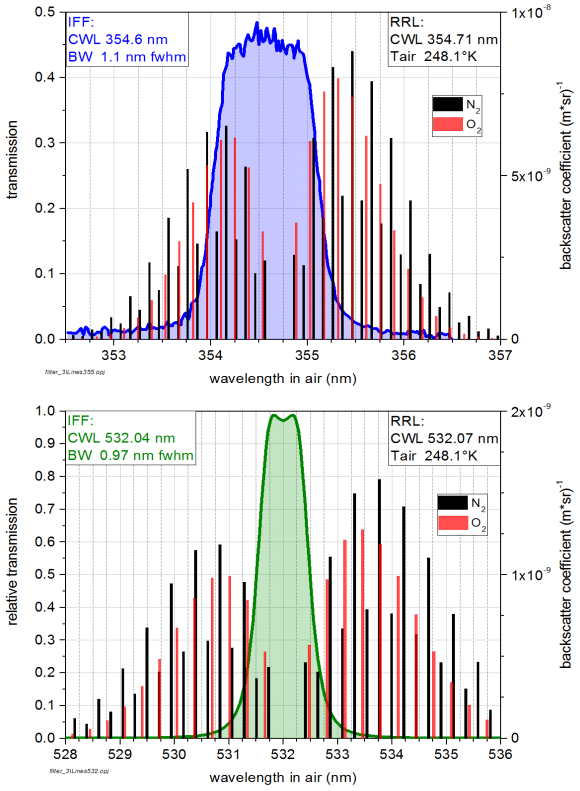

Figure 3 Rotational Raman lines (RRL, backscatter coefficient, right scale) of N_2 and O_2 at 248 K air temperature (central line omitted) and the transmission of the used interference filters (IFF) (see Table 1 for BW and CWL).

We calculate the backscatter coefficients of individual RRLs of N_2 and O_2 (Fig. 3) at different air temperatures according to [7, 8] and weight them with the IFF transmissions for the sum of their

LDRs (see Fig. 4).

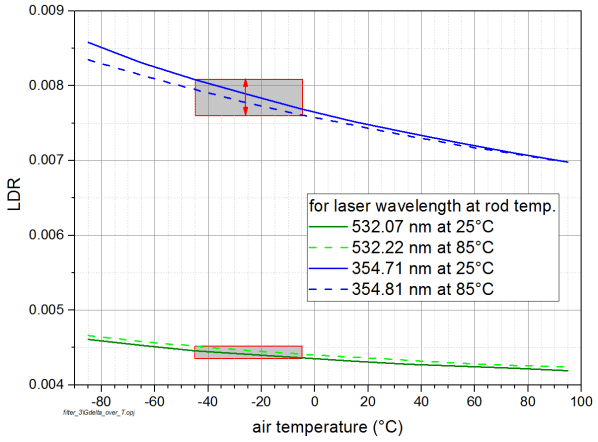

Figure 4 Theoretical LDRs of clean air (with 385 ppmv CO_2 and 0% RH) over air temperature including the rotational Raman lines of O_2 and N_2 within the used IFF bandwidths and considering laser wavelength ranges for rod temperatures between 25°C and 85°C. The red rectangles show the considered variability of air temperature and laser wavelength, and the red arrow the resulting uncertainty of the theoretical LDR.

4. MEASUREMENTS

POLIS-6 was first deployed during a one-month field campaign in 2013. At several nights, measurements of assumed clean air ranges above the aerosol layers were possible with sufficient high signal-to-noise ratios after temporal averaging. With temporal close Δ90°-calibration measurements it was possible to determine the calibration factor and from that the calibrated signal ratio δ^* [2, 3] with an accuracy better than ±2%, and to estimate the rotation ε between the plane of polarization of the laser beam and the receiving optics [2] (see Fig. 5). The corrected LDRs (δ) calculated from Eq. (1) [2] are shown in Fig. 6 together with the error bars, derived with Eq. (2).

$$\delta = \frac{1+D_O}{1-D_O}\frac{\delta^* - \tan^2\varepsilon}{1-\delta^*\tan^2\varepsilon} \quad (1)$$

$$|\Delta\delta| \approx \frac{1+D_O}{1-D_O}\left(|\Delta\delta^*| + |2\varepsilon\Delta\varepsilon|\right) \quad (2)$$

After initial system adjustments until 25.06.13, the uncertainty due to Δε becomes negligible compared to Δδ*; the latter mainly stems from signal noise. For the period after 25.06. the mean LDRs are $\overline{\delta}$ = [0.0083, 0.0054] and the mean

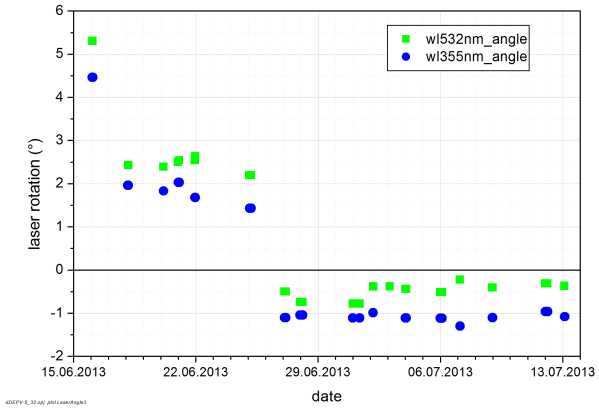

Figure 5 Rotation between the plane of polarization of the laser beam and the incidence plane of the receiving optics (laser rotation) determined with the Δ90°-calibration.

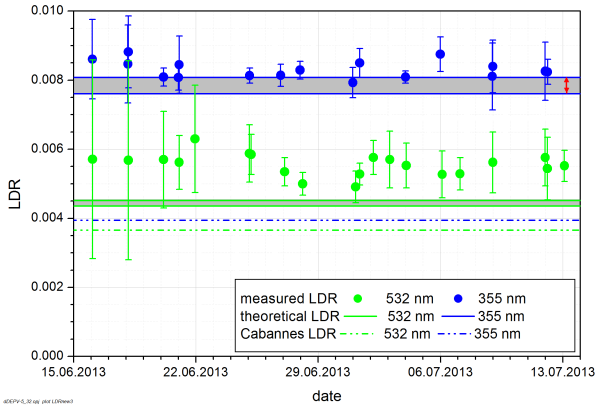

Figure 6 Linear depolarization ratios (LDR) of presumable clean air ranges measured during SALTRACE with POLIS-6 at 355 and 532 nm (dots). The dash-dotted lines show the theoretical LDR if only the central Cabannes line passes the IFF, and the gray areas between solid lines show the theoretical ranges from Fig. 4.

uncertainties $\overline{\Delta\delta}$ = [4.8e-4, 5.9e-4] at [355, 532] nm, respectively. The theoretical LDRs (gray areas in Figs. 4 and 6) range between 0.00761 and 0.00808 at 355 nm, and between 0.00436 and 0.00452 at 532 nm, which means that the measured values are about 0.0005 and 0.0012 higher at 355 and 532 nm, respectively.

It is remarkable in Fig. 5 that the difference between the laser rotation at 355 and 532 is about 0.5° over the whole campaign, with a variability well explainable by signal noise.

5. CONCLUSIONS

We show that it is possible to measure the linear depolarization ratio of clean air with a lidar with high accuracy, if polarizing optics in the emitter and receiver (before the polarizing splitter) are avoided, if the cross talk of the polarizing splitter is suppressed, if the simple but high accurate Δ90°-calibration with mechanical rotation is used, and if the plane of the laser polarization is well aligned with the incidence plane of the receiving optics. At this accuracy level it becomes necessary to include in the calculation of the molecular linear depolarization ratio the influence of the rotational Raman lines within the interference filter bandwidth and to account for the uncertainty of the laser wavelengths due to the unknown laser rod temperature. Furthermore, we find a difference in the rotation of the plane of polarization of about 0.5° between the second and third harmonic of the employed laser, which might be caused by the third harmonic generator, because this is the only optical component between the second harmonic generator and the Δ90°-calibrator. While the difference between the measured and theoretical LDR at 355 nm is only about 0.0005 with a mean measurement uncertainty in the same range, the difference is 0.0012 at 532 nm with an uncertainty of about 0.0006. Possible reasons are residual aerosol in the assumed clean air range, or/and elliptical polarization of the 532 nm due to the third harmonic generator.

REFERENCES

[1] Reichardt, J., R. Baumgart, T. McGee, 2003: Three-Signal Method for Accurate Measurements of Depolarization Ratio with Lidar, *Appl Opt,* **42 (24)**, 4909-4913.

[2] Freudenthaler, V., 2015: Polarisation sensitivity of lidar systems and the Δ90°-calibration, *in preparation for AMTD.*

[3] Freudenthaler, V., M. Esselborn, M. Wiegner, B. Heese, M. Tesche, A. Ansmann, D. Müller, D. Althausen, M. Wirth, A. Fix, G. Ehret, P. Knippertz, C. Toledano, J. Gasteiger, M. Garhammer, M. Seefeldner, 2009: Depolarization ratio profiling at several wavelengths in pure Saharan dust during SAMUM 2006, *Tellus B,* **61 (1)**, 165-179.

[4] Freudenthaler, V., 2003: Optimized background suppression in near field lidar telescopes, http://epub.ub.uni-muenchen.de/12957/

[5] Kushida, T., 1969: Linewidths and Thermal Shifts of Spectral Lines in Neodymium-Doped Yttrium Aluminum Garnet and Calcium Fluorophosphate, *Phys. Rev.,* **185** , 500-508.

[6] Kaminskii, A., 1990: Laser Crystals, *Springer Berlin Heidelberg.*

[7] Behrendt, A., 2005: Temperature Measurements with Lidar, in Weitkamp, C. (ed.): Lidar, *Springer New York*, 2005, 273-305.

[8] Wandinger, U., 2005: Raman Lidar, in Weitkamp, C. (ed.): Lidar, *Springer New York*, 2005, 241-271.